8. Impact of Climate Change and Sea Level Rise on Storm Surges

The ideas of Global Change and the Greenhouse Effect are usually interpreted narrowly, in the sense of anthropogenic causes of warming of the earth and climatic change. In reality, the predicted warming of the earth is due to the Greenhouse Effect. However, this is not exclusively a phenomenon of the present, in particular the time since the Industrial Revolution, but, rather, a natural response of the earth and its atmosphere to solar radiation.

The natural Greenhouse gases ensure that the climate remains pretty much constant and that an average temperature between +15° C and –15° C predominates on earth, since they permit the warming sunlight to permeate to the earth and, on the other hand, prevent the thermal radiation from the earth from completely escaping into space. The earth's equilibrium radiation balance is composed of a combination of the following components (GRASSL and KLINGHOLZ, 1990).

An output of 343 Watts reaches each square metre of the earth's surface. Of this, clouds, the brightness of the earth's surface and air molecules reflect 30 %. Opposing this, 49 % of the sun's radiation is absorbed by the earth's surface and 30 % by the atmosphere. This energy also warms the earth and, among other things, causes water to evaporate from the oceans. The earth, in turn, radiates the afore mentioned thermal energy outwards. However, a part is held back because of the clouds and the Greenhouse gases. Whilst the visible sun's energy reaches the earth as short-wave radiation, and thereby penetrates through the earth's atmosphere, the earth in turn emits long-wave radiation.

Carbon dioxide is used here as an example of the Greenhouse gas molecules to explain the "functioning" of the Greenhouse gases. When the thermal radiation hits a carbon dioxide molecule, the oxygen atoms on the side of the carbon begin to rotate and induce the carbon atom to vibrate. In this manner, the carbon atom absorbs the thermal radiation and heats up the atmosphere. A part of the energy that is given off in all directions by the carbon dioxide molecules will be returned to the earth.

The other Greenhouse gases, mainly water vapour, ozone, laughing gas, methane and the anthropogenically-produced chlorofluorocarbons, have a similar effect, so that only 16 % of them will be transmitted to the space directly; the rest will be transmitted through the atmosphere. In this manner a balance arises, which means that out of the 237 W/m^2 of solar energy, which reaches earth, 390 W/m^2 of the thermal radiation will be returned to the atmosphere. However, only the "equivalent" 237 W/m^2 disappears into space the remaining 153 W/m^2 will be emitted again and again, ultimately leaving the earth in equilibrium, as a result of the Greenhouse gases. In this manner the Greenhouse gases operate like a pane of the greenhouse. The climate system, like all complex systems, will be variable, as would also be the case without anthropogenic intervention, "depending on the most dominant timescale of the interacting parts of the climatic fluctuations involved. It is then only a question of the average time intervals chosen as to whether the variability of the climatic fluctuations will be significant" (GRASSL, 1993).

8.1 The Greenhouse Gases

Water vapour, carbon dioxide, methane, ozone and nitrogen dioxide are Greenhouse gases. In combination they make up an extremely small portion of the air. Dry air – dry due to the very variable portions of water vapour in the air – consists of up to 78.08 % nitrogen, up

to 20.95 % of oxygen and up to 0.93 % of the inert gas argon (GRASSL and KLINGHOLZ, 1990), none of which have any relevant role with regard to the terrestrial thermal equilibrium. These components lack the necessary characteristics to absorb solar radiation and thermal radiation.

As already mentioned, the most important Greenhouse gas affecting the heat balance is water vapour. It varies, depending on temperature and air humidity, in its volumetric proportion from one million parts in the stratosphere (the layer of the atmosphere about 50 km above the earth) to over one thousand parts over the polar regions and up to 300 parts in the tropics near the earth's surface (GRASSL and KLINGHOLZ, 1990).

Carbon dioxide, although one of the most important gases in the air only makes up 0.035 % of the air, but next to water vapour, is one of the most important Greenhouse gases. All Greenhouse gases combined make up, in total, only 3 % by volume of the air.

Table 8.1: A sample of Greenhouse gases affected by human activities (IPCC, 1995)

	CO_2	CH_4	N_2O	CFC-11	HCFC-22 (CFC-substitute)	CFC_4 (perfluoro-carbon)
pre-industrial concentration	280 ppmv	~ 700 ppbv	~ 275 ppbv	0	0	0
Concentration 1994	358 ppmv	1720 ppbv	312* ppbv	268* pptv	110 pptv	72* pptv
Rate of change of concentration*	1.5 ppmv/yr 0.4 %/yr	10 ppbv/yr 0.6 %/yr	0.8 ppbv/yr 0.25 %/yr	0 pptv/yr 0 %/yr	5 pptv/yr 5 %/yr	1.2 pptv/yr 2 %/yr
Atmospheric life time	50–200§§	12§§§	120	50	12	50.000

The growth rates of CO_2, CH_4 and N_2O are averaged over the decade commencing 1984; halocarbon growth rates are based on recent years (1990s).

* = Estimated from 1992–93 data.

§ = 1 pptv = 1 part per trillion (million million) by volume.

§§ = No single lifetime for CO_2 can be defined because of the different rates of uptake by different sink processes.

§§§ = This has been defined as an adjustment time which takes into account the indirect effect of methane on its own lifetime.

CFC = Chlorofluorcarbon.

Tab. 8.1 shows the increase of Greenhouse gases due to anthropogenic activity. The figures are taken from the 1995 IPCC report (IPCC, 1995). Clearly, a rise in the concentration of CO_2 has been recorded from 280 ppmv in pre-industrial times to 358 ppmv in 1994. Equally, there is no doubt that this rise is connected with anthropogenic activity, especially the burning of fossil fuels, but also with alterations to the use of land and, to a lesser degree, concrete production. Before the rise in the concentration of CO_2, CO_2 concentration fluctuated about 280 ppmv ±10 ppmv for around 1000 years.

In addition, methane rose, doubtless due to anthropogenic activity, such as rice cultivation, animal husbandry, burning of biomass and gas leakage, as well as the use of fossil fuels. The global average methane concentration has risen by about 6 % in the decade since 1984 and by about 145 % between the Industrial Revolution and 1994.

N_2O (nitrogen dioxide, laughing gas) has a relatively low rate of increase, but, for all that, a long residence time in the atmosphere. The cause of laughing gas is, above all, nitrogenous manure in the landscape and a succession of industrial processes. Since the Industrial Revolution, the proportion of N_2O in the atmosphere has risen from 275 ppv to 312 ppv, in association with a clear decrease in the growth rate in recent years (in the 80s and early 90s close to 0.8 ppbv/year, reducing to 0.5 ppbv/year in 1993).

In the early 90s, the growth rate of CO_2, CH_4 and N_2O was insignificant. This natural variation is still not clear, but the data from recent years show that the trend of the 80s is continuing.

Halocarbons include chlorine and bromine and result in ozone depletion. The Montreal Protocol sets limits on emissions, as a result of which the growth rate has been reduced. The growth rate of CFC_s has, as a result, been reduced to zero. The Montreal Protocol also ordered reductions in the concentration of CFC_s, $HCFC_s$ and their consumption of ozone.

Greenhouse gases with longer duration times, such as, mainly, $HCFC_s$, PFC_s and SF_6, are currently an insignificant influence on radiation intensity. However, their projected growth may greatly increase the intensity of radiation amplification in the twenty-first century.

Ozone, O_3, is an important Greenhouse gas, present in both the stratosphere and the troposphere. Alterations to ozone result in increased radiative forcing by influencing both the solar incoming radiation and the outgoing terrestrial radiation. The intensity of the solar radiation is strongly related to the vertical distribution of ozone and reacts with particular sensitivity to alterations at the level of the troposphere. The pattern of tropospheric and stratospheric ozone alterations is spatially variable. The estimation of the radiative forcing due to changes in ozone is essentially more complicated than that for the Greenhouse gases.

Tropospheric ozone levels have clearly risen since 1900, with strong evidence that this has occurred in many places since the 60s. In the 1990s, however, the upward trend has slowed and almost come to a halt. Altogether the northern hemisphere has seen a doubling in tropospheric ozone since the Industrial Revolution, an increase of 25 ppbv; whereas, in the southern hemisphere a diminution has been recognised since the mid-80s.

Decreases in stratospheric ozone have been observed since the 70s, mainly in the lower stratosphere, the most obvious feature of which is the phenomenon of the ozone hole over the Antarctic in September and October. A statistically significant decrease in total ozone levels has been noted in the mid latitudes of both hemispheres. In the tropics there is a slight trend towards ozone reduction, rather than an increase.

The calculation of the global average radiative forcing is a good way to get an overall impression of the potential climatic relevance of the individual components. Looking at this from a global angle has limitations:

1. the spatial pattern of the mixture of Greenhouse gases
2. the regional variation of tropospheric ozone and
3. the regional variation of tropospheric aerosols.

Such a global view of the radiative forcing does not reflect the complete pattern of potential climatic variations. It is not permitted to take negative numbers into account as a balancing factor. Table 8.2 presents the average radiative forcing:

Table 8.2: Annually Average Radiative Forcing

Factors	Capacity in Wm^{-2}
Greenhouse gases (CO_2, CH_4, N_2O and Halocarbons)	+ 2.45 Wm^{-2} (from + 2.1 to + 2.8 Wm^{-2})
Tropospheric ozone	+ 0.4 Wm^{-2} (from + 0.2 to + 0.6 Wm^{-2})
Stratospheric ozone	– 0.1 Wm^{-2} (from – 0.05 to – 0.2 Wm^{-2})
Anthropogenic Aerosols (Sulphates, soot from fossil fuel, mainly coal, and organic aerosols resulting from biomass burning)	– 0.5 Wm^{-2} (from – 0.25 to – 1.0 Wm^{-2})
Sulphate aerosols (fossil fuel emission)	– 0.4 Wm^{-2} (from – 0.2 to – 0.8 Wm^{-2})
Soot in aerosols from fossil fuel sources	+ 0.1 Wm^{-2} (from 0.03 to 0.3 Wm^{-2})
Direct radiative forcing of particles associated with biomass burning	– 0.2 Wm^{-2} (from – 0.07 to –0.6 Wm^{-2})
Tropospheric dust particles influenced by man's activities	not quantifiable
Changes in cloud properties caused by aerosols due to man's activities (indirect effect)	0 to – 1.5 Wm^{-2} (cannot be quantified exactly, which is why, for scenario as a rule, –0.8 Wm^{-2} is used)
Alterations to radiative forcing due to changes in solar radioactive output*	+ 0.3 Wm^{-2} (from 0.1 to 0.5 Wm^{-2}) since 1850
Aerosols resulting from volcanic eruptions*	large for short periods of time (few years), e.g. Mt. Pinatubo –3 to –4 Wm^{-2}

* The past variation can explain climatic changes of periods of time on a decadal basis.

8.2. Global Change

As is seen clearly from the above, changes in global climate are closely correlated with the amount of Greenhouse gases in the atmosphere. In the case of an increase of Greenhouse gases in the atmosphere, the air temperature on earth will also rise, and this, in turn, will stimulate the earth's hydrological cycle: "per degree of temperature change, the amount of water vapour in the air increases by about 10 %" (GRASSL, 1993: 29). It has to be pointed out that the Greenhouse gases are always efficacious at a global scale and cannot be compensated on a regional basis, unlike the anthropogenic alterations of the surface (GRASSL, 1993).

A further feedback arises through alterations of temperature in the hydrological cycle. These temperature variations occur due to the fact that the brightest and darkest natural surfaces of the Earth are constituted of water. The darkest surface is the ocean and powdery snow is the brightest. In the case of warming, the brightness of the surface decreases and it will absorb more solar energy; this means that a further warming will result from the melting of the glaciers.

The clouds, as an additional factor, have two effects: whilst the low clouds mainly have a cooling effect, the high clouds have a warming effect. These thin high clouds are, however, also created by anthropogenic effects through aircraft exhaust emissions. However, the ultimate effect of the clouds on global warming is, currently, not clear.

The mean global surface temperature has risen by about 0.3° to 0.6° C since the late 19th century, and by about 0.2° to 0.3° C over the last 40 years. The warming occurred largely during two periods, between 1910 and 1940 and since the mid-1970s (IPCC, 1995).

The warming has not been globally uniform. The recent warmth has been greatest over the continents between 40° N and 70° N. A few areas, such as the North Atlantic Ocean north of 30° N, and some surrounding land areas, have cooled in recent decades (IPCC, 1995).

It can, however, be pointed out that since 1400 AD the global average temperature has been higher than in all previous centuries during the historic period (IPCC, 1995).

However, this cannot be clearly differentiated from the natural variations of the climate due to the alterations of trace gas concentration since the beginning of the Inertia Revolution, as the uncertainty in the key factors is still too great and the thermal of the ocean to balance the retardation of the effects of the previous influence of each decade have to be considered.

Information on **climatic change in the future** is much more difficult to ascertain, as the main problem lies in the estimation of future anthropogenic trace gas emissions. Therefore different scenarios have been undertaken, which take into account the differing increases in trace gas emissions. Data from the Intergovernmental Panel on Climate Change (IPCC) have been used as a basis for the production of these scenarios. This Panel was founded as an intergovernmental committee and is supposed to be used as the basis for political decisions. However, it must be noted that other institutions sometimes predict a different set of results.

The IPCC differentiates between four scenarios, which are calculated from coupled ocean-atmosphere models. These scenarios, whose assumptions are listed below, take into account the emissions from Greenhouse gases as well as aerosol processes:

A) Economic development remains as at present, so that the world energy consumption quadruples to the year 2100. At the same time the rate of cutting of the tropical rainforests continues as before (Scenario "Business As Usual").
B) Moderate intervention in the global trace gas exchange will occur.
C) Considerable intervention in the global trace gas exchange will occur.
D) An immediate and considerable reduction in the ejection of all climatically significant trace material will occur. In spite of this, all Greenhouse gases initially increase in this scenario until the year 2030.

Equally in the case of – as GRASSL and KLINGHOLZ (1990) (in translation) put it so well – "an immediate and complete cessation" there would be a definite rise in the global average temperature over the next 100 years. The clearest conclusion comes, naturally, from Scenario A "Business As Usual", as a result of which the most favourable outcome for man would be a temperature increase of 2.0° C by 2100, followed by a continued rise with hardly any reduction in rate. "Such a high average temperature has not occurred since at least 200 000 years ago" (GRASSL, 1998). There is, essentially, a slight reduction in the increase for Scenarios B and C. The likely equilibrium response of global surface temperature to a doubling of equivalent carbon dioxide concentration (the "climate sensitivity") was estimated in 1990 to be in the range 1.5 to 4.5° C, with a "best estimate" of 2.5° C (IPCC, 1995).

Although CO_2 is the most important Greenhouse gas, the other Greenhouse gases contribute a significant portion (30 %) the projected global warming.

8.2.1 Effects

The results of such an increase in temperature would be quite varied and broad. In general, an increase of temperature of just one tenth of a degree would alter the boundary of the deserts by 50–100 km; half a degree would displace the northern forest boundaries by the same distance and cause the glaciers of the mid latitudes to retreat by a vertical distance of at least 200 meters. "The Earth has not experienced a 2 degrees higher average temperature since the existence of modern man, Homo sapiens. A four degrees warmer Earth has not occurred since man first appeared four million years ago" (GRASSL and KLINGHOLZ, 1990).

The following effects for temperature and precipitation may be ascertained from the models (IPCC, 1995):

"All model simulations, whether they are forced with increased concentrations of greenhouse gases and aerosols, or with increased greenhouse gas concentration alone, show the following features:

- generally greater surface warming of the land than of the oceans in winter, as in equilibrium simulations;
- a minimum warming around Antarctica and in the northern North Atlantic which is associated with deep oceanic mixing in those areas;
- maximum warming in high northern latitudes in later autumn and winter associated with reduced sea ice and snow cover;
- little warming over the Arctic in summer;
- little seasonal variation of the warming in low latitudes or over the southern circumpolar ocean;
- a reduction in diurnal temperature range over land in most seasons and most regions;
- an enhanced global mean hydrological cycle;
- increased precipitation in high latitudes in winter.

"Including the effects of aerosols in simulations of future climates leads to a somewhat reduced surface warming, mainly in the mid latitudes of the Northern Hemisphere. The maximum winter warming in high northern latitudes is less extensive.

"However, adding the cooling effect of aerosols is not a simple offset to the warming effect of greenhouse gases, but significantly affects some of the continental-scale patterns of climate change. This is most noticeable in summer where the cooling due to aerosols tends to weaken monsoon circulations. For example, when the effects of both greenhouse gases and aerosols are included, Asian summer monsoon rainfall decreases, whereas in earlier simulations with only the effect of greenhouse gases represented, Asian summer monsoon rainfall increased.

"Conversely, the addition of aerosol effects leads to an increase in precipitation over southern Europe, whereas decreases are found in simulations which employ only the greenhouse gases." (IPCC, 1995).

"All model simulations, whether they are forced with increased concentrations of greenhouse gases and aerosols, or with increased greenhouse gas concentration alone, produce predominantly increased soil moisture in high northern latitudes in winter. Over the northern continents in summer, the changes in soil moisture are sensitive to the inclusion of aerosol effects." (IPCC, 1995:43).

8.2.2 Ocean circulation

"In response to increasing greenhouse gases, most models show a decrease in the strength of the northern North Atlantic oceanic circulation further reducing the strength of the warming around the North Atlantic. The increase in precipitation in high latitudes decreases the surface salinity, inhibiting the sinking of water at high latitude, which drives this circulation." (IPCC, 1995).

The alterations of the regional gradients are, as a rule, greater than the global gradients, because the amount of aerosols, the land use and the combined ecological effects of the individual factors can amplify or, depending on circumstances, can also reduce the variation.

The variability of the climatic change has a greater effect than the equivalent changes in average climate variations. They can lead to alterations in the frequency of extremes (IPCC, 1995):

8.2.3 Temperature

A general warming tends to lead to an increase in the occurrence of extremely high temperatures and a decrease in extremely low temperatures (e.g., frost days).

8.2.4 Hydrology

New results reinforce the view that variability associated with an enhanced hydrological cycle translates into prospects of more severe droughts and/or floods in some places and less severe droughts and/or floods in other places.

8.2.5 Mid-latitude storms

Conclusions regarding extreme storm events are, obviously, even more uncertain.

8.2.6 Hurricanes/Tropical cyclones

Although some models now represent tropical storms with some realism for present day climate, the state of the science does not allow assessment of future changes.

8.2.7 El Nino-Southern Oscillation

An average warming of the sea surface in the tropics will result from increased Greenhouse gas emissions, so the variability of the precipitation could be increased, as occurs in connection with ENSO events.

8.3 Sea-Level Rise

One of the major consequences of climate change could be the rise of sea level.

There are hundreds of publications about this phenomenon, these can be distinguished between those, which focus their research on the postglacial sea-level rise, and those, which look at the changes over the last 100 years and calculate future trends.

This chapter concentrates on the second approach. The results and conclusions refer to IPCC 1995, except where indicated to the contrary.

8.3.1 Reasons for Sea-Level Rise (GRASSL, 1993)

In the case of global warming, the sea level will rise. There are mainly two reasons for this reaction to the rise of temperature. Firstly the thermal expansion of the oceans, secondly melting of mountain glaciers. The two other big potential resources of water for sea-level rise are the Antarctic and the Greenland ice sheets.

Thermal expansion of water depends on the depth of the warming of the water body and the ocean currents. Therefore the thermal expansion results in a regional pattern of sea-level rise and global estimation is very difficult. It is certain that areas of the ocean, which are mixed in depth, will have a greater thermal expansion in relation to the warming of the surface.

By contrast, melting of the ice sheets cause a sea-level rise, which results in the same alterations in level globally. Whereas the mountain glaciers can cause a global sea-level rise the reaction of the ice sheet from Greenland cannot be calculated very well, because the answer to the question as to whether it is melting or expanding is not certain.

The IPCC (1995) summarises the function of the Greenland and Antarctic ice sheets as being relatively minor over the next century. However, the possibility of large changes in volumes of these ice sheets (and consequently, in sea-level) cannot be ruled out, although the likelihood is considered low. (IPCC, 1995)

8.3.2 Has Sea-Level Risen? (IPCC, 1995)

The analyses of tide gauge records show a sea-level rise by about 10–25 cm over the last 100 years. The main uncertainty of results from tide gauges is the vertical land movement, but methods for filtering out the effects of long-term vertical land movements as well as greater reliance on the longest tide-gauge records for estimating trends have given greater confidence in the results.

Over the period of the last 100 years much of the sea-level rise has been related to the concurrent rise in the global temperature. The observed sea-level rise may account initially for about 2 to 7 cm from the warming and consequent expansion of the oceans and secondly for about 2 to 5 cm from the retreat of glaciers and ice caps. "Only a small change in sea-level has been caused by surface and groundwater storage."

"The rate of observed sea-level rise suggest that there has been a net positive contribution from the huge ice sheet of Greenland and Antarctica, but observations of the ice sheets do not yet allow meaningful quantitative estimates of their separate contributions. The ice sheets remain a major source of uncertainty in accounting for past changes in sea-level, because there are insufficient data about these ice sheets over the last 100 years." (IPCC, 1995) Furthermore is not really clear if they cause a sea-level rise or decrease (GRASSL, 1993).

8.3.3 Global mean Sea-Level Projections

Projections of the global sea-level rise are taken from the results of IPCC 1995: Summary and 40 ff.; for the calculation for the 21st century IS92 scenarios are used. "For the IS92a scenario assuming the "best estimate" values of climate sensitivity and of ice melt sensitivity to warming, and including the effects of future changes in aerosol, models project an increase of sea-level of about 50 cm from the present to 2100." (IPCC, 1995). The range between the lowest emission scenario (IS92c) and the highest emission scenario (IS92e) is 15 cm to 95 cm from present to 2100 (Fig. 8.1).

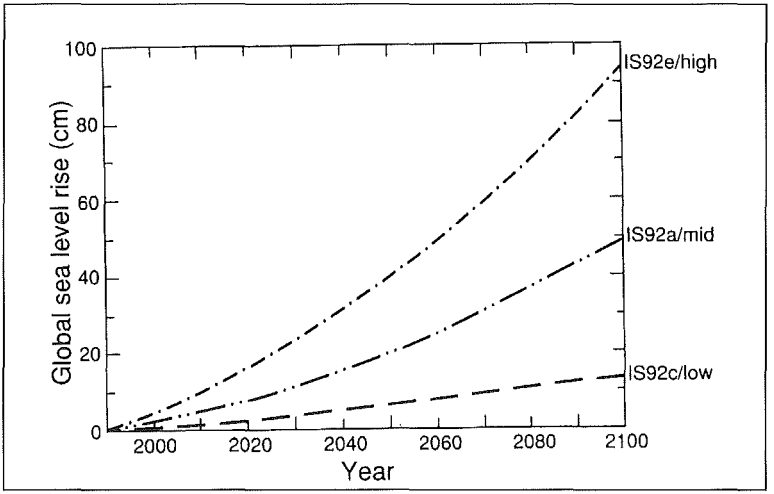

Fig. 8.1: Projected global mean sea-level rise extremes from 1990 to 2100. The highest sea-level rise curve assumes a climate sensitivity of 4.5° C, high ice melt parameters and the IS92e emission scenario; the lowest a climate sensitivity of 1.5° C, low ice melt parameters and the IS92c emission scenario and the middle curve a climate sensitivity of 2.5° C, mid-value ice melt parameters and the IS92a scenario (IPCC, 1995)

Due to the large thermal inertia of the ocean-ice-atmosphere climate system the choice of emission scenario has relatively little effect on the projected sea level rise. In the second part of the 21st century the effects increase.

Moreover the sea-level "would continue to rise at a similar rate in future beyond 2100, even if concentrations of greenhouse gases were stabilised by that time, and would continue to do so even beyond the time of stabilisation of global mean temperature." (IPCC, 1995)

The future sea-level rise will differ regionally owing to regional differences in heating and circulation changes.

8.4 Possible Impact on the Intensity and Frequency of Cyclones

One of the widely recognized consequences of global warming would be increased sea surface temperature (SST). It is known that the tropical cyclones derive their energy mainly from the latent heat of evaporation from the ocean. Warm water of at least 26–27° C is needed to supply energy for cyclogenesis. The behaviour of tropical cyclones in warmer world, where we may have larger area of sea having temperature over this critical value, has been the subject of considerable speculation and concern.

Although the casual relationship between SST and the formation of tropical cyclones suggest that the theoretical maximum intensity may increase with temperature, the evidence inferred from several observational and modelling studies is still conflicting (RAPER, 1993; RYAN et al., 1992; STEIN and HENSEN, 1994). This may be attributed to the fact that the formation of tropical cyclones depends not only on SST but a number of other factors which include, the vertical lapse rate of the atmosphere, vertical wind shear, mid-tropospheric relative humidity and the prior existence of a center of low-level cyclone vorticity (GRAY, 1979). The factors change in complex ways with changing climate. An estimate of such changes is therefore not straightforward and may only be derived from state-of-the-art climate models. Present day climate models are able to simulate some of the aspects of tropical cyclone occurrence (MANABE and BROCCOLI, 1990; HAARSMA et al., 1993), they are not adequate enough to predict changes in warming climate. Most of the impact assessment studies carried so far use indirect techniques, rather than direct simulation of the tropical cyclones.

EMANUEL (1987) combined the CO_2 induced SST changes simulated by the Goddard Institute of Space Studies (GISS) climate model (HANSEN et al., 1984) with a theoretical tropical cyclone model (EMANUEL, 1986) to estimate the potential change in the intensity of tropical cyclones. His estimate showed that the intensity of tropical cyclones would increase as a result of increased tropical SSTs. However, in the absence of any empirical evidence in this regard. Emanuel's modelling results may not be considered very realistic.

NICHOLLS (1989) examined the activities of tropical cyclones and their intensities with SST from observations. He found little evidence of any relationship between monthly average SST and the number of tropical cyclones.

RAPER (1993) studied in detail the relationship between climate change and the frequency and intensity of severe tropical cyclones for the six tropical cyclogenesis regions, viz., North Atlantic, Western North Pacific, Eastern North Pacific, North Indian and extended Australian region (Southwest Pacific/Australian region). He used the US National Oceanic and Atmospheric Administration tropical cyclone data set (NOAA, 1988) for his study. He did not find any convincing empirical evidence in support of the relationship between SSTs and cyclone intensities. However, an increase in SSTs indicated a threshold effect that could lead to increase in the intensity of most severe storms. With regard to the relationship between tropical cyclone activity and SSTs, RAPER (1993) found different relationships in different areas. While predominantly negative correlation is found in two (North Indian Ocean and West North Pacific) of the six cyclone regions, four other regions showed a predominantly positive correlation. In the regions with highest positive correlation, simple regression suggests an increase of 37–63 % in severe tropical storm frequency per degree increase in SST. However, this relationship may not be constructed as having predictive skill for long term climate change as evidence suggest that the relationship is not necessarily directly casual because the areas of correlation are not always coincident with the areas of cyclone origin and tracks. Thus, the effect of SSTs may be indirect, through the connection with the regional-

scale atmospheric circulation. The main conclusion emerged from the analysis of RAPER (1993) was that changes in tropical cyclone activity in warmer world will depend crucially on the changes that may occur in the regional-scale atmospheric circulation.

A study undertaken by GRAY (1990) suggests that Atlantic hurricane activity over the period 1970 to 1987 was less than half that in the period 1947 to 1969, Western North Pacific also showed a decrease in the number of very intense tropical cyclones. In the Northeast and Southwest Pacific the number of cyclones appears to have increased (THOMPSON et al., 1992; LANDSEA et al., 1996).

EVANS (1993) looked into the relationship between SST and intensity of TCs for different regions where they form. Except for intense storms in the North Atlantic, his results indicate that there is little evidence to support the direct relationship between SSTs and cyclone intensities in most of the regions. CHANGNON (1993) studied historical variations in 146 major storms during 1950–1990 to describe their temporal characteristics and possible relationship to climate change. His results suggest that a warmer regime over North America would be associated with a greater incidence of major storms in the US.

In the North Indian Ocean the frequency of tropical disturbances has noticeably decreased (GADGIL, 1995) since 1970 (Fig. 8.2) while SSTs have risen here since 1970, probably more than in any other region (RAPER, 1993).

PITTOCK (1992) reports that sensitivity studies using limited area models in response to modelled increase in SST, suggests that cyclones may be more intense under warmer conditions. He notes, however, that historical data do not demonstrate any strong link between tropical cyclone numbers or intensity and SST, other than the lower limit for occurrence of around 27° C.

LIGHTHILL et al. (1994) observed that although substantial regional changes are expected but there are no compelling reasons to believe a major change in global tropical cyclone frequency.

As mentioned earlier, present day climate models are not able to simulate tropical cyclones well, nevertheless there have been large numbers of modelling studies carried out using low resolution GCMs. RYAN et al. (1992) used a GCM to assess tropical cyclone frequencies from yearly Genesis Parameter defined by GRAY (1975). He showed that the Gray's parameter forced by the output of a GCM gives a good representation of the observed tropical cyclone climatology. He, however, notes that changes in the Gray's Genesis Parameter due to enhanced greenhouse conditions were dominated by the SST changes.

In another numerical experiment carried out with the GFDL coupled ocean-atmosphere model, STEPHENSON (1993) showed that the Atlantic storm track weakens with increasing CO_2, while the Pacific storm track changes little. HAARSMA et al. (1993) analyzed the results of a GCM to show that the number of simulated tropical disturbance increases by about 50 % with the doubling of the CO_2 concentration. His GCM analysis also indicated a change in cyclone tracks as a result of CO_2 induced global warming. On the other hand, BENGTSSON et al. (1994) indicated that with a doubling of CO_2 over the next 50 years, the global and seasonal distribution of storms should be similar to the present observations. They also found a significantly reduced number of tropical cyclones for enhanced greenhouse scenario. This decrease in the number of tropical cyclones was substantial in the Southern Hemisphere, which seems unusual.

Recently DRUYAN and LONERGAN (1997) adapted hurricane frequency index (GRAY, 1979) so that it can be computed from simulations by the NASA/GISS climate model. Based on simulation experiments, they found that an atmosphere with double the present concentrations of CO_2 could lead to an increase of about 50 % in the number of tropical storms

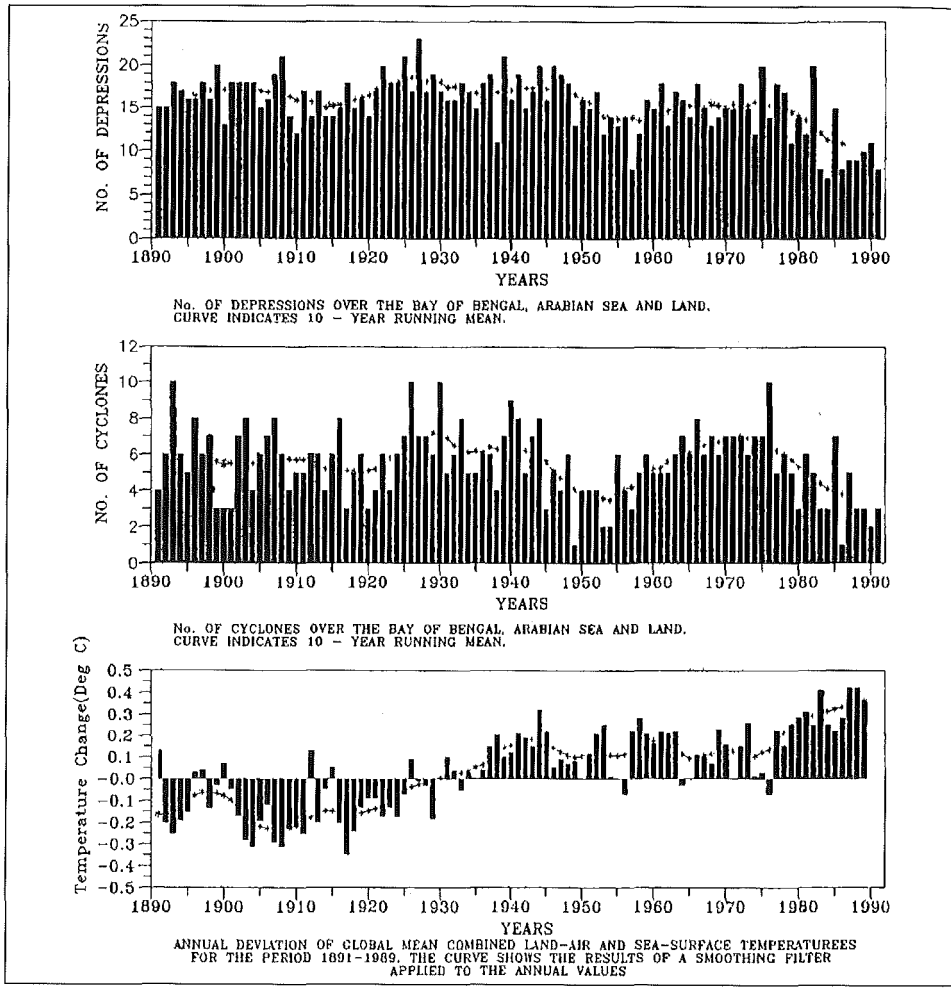

Fig. 8.2: Variation of the frequency of depressions and cyclones over the Indian seas (GADGIL, 1995)

(winds exceeding 64 km/h) and hurricanes that form over the Gulf of Mexico, and an increase of more than 100 % over the tropical North Pacific Ocean.

More recently WALSH and PITTOCK (1998) indicate that because of the insufficient resolution of climate models and their generally crude representation of sub-grid scale and convective processes, little confidence can be placed in any definite predictions of potential changes in tropical storms as a result of climate change. However, a tendency for more heavy rainfall events seems likely, and a modest increase in tropical cyclone intensities is possible. In the views of the author, it would be unwise to exclude substantial local changes in the climatologies of these phenomena, especially at regional (sub-continental) scale.

In the end we can say that the formulation and intensification of tropical cyclones depend not only on SST but also on a number of atmospheric factors. The tropical cyclone activity in a warmer world will, therefore, depend on regional changes that may occur. In the absence of the models that may adequately predict these regional changes, it is not possible to make future projections for changes in global tropical cyclone frequency and intensity.

8.5 ENSO and Tropical Cyclone Activity

8.5.1 Impact on Tropical Cyclone Frequency

The role of environmental or external forcing processes on tropical cyclone formation, structure, structural change and motion has been known and accepted in varying degrees by meteorologists for many years. El-Nino/Southern Oscillation (ENSO) is the most important short-term climatic fluctuation of tropical circulation. In recent years its possible role in modulating tropical cyclone activities in different parts of the world has been emphasized (GRAY, 1984a).

The pioneering work in this field was by NICHOLLS (1979, 1984, 1985) for cyclones in the two Australian basins. He demonstrated an association between the Southern Oscillation Index (SOI) during the Southern Hemisphere winter and the number of tropical cyclones close to Australia (from 105–165 E) during the subsequent cyclone season (i.e., from October to April). The number of cyclone days over a season is correlated with mean sea-level pressure for the preceding July–September. The linear correlation coefficient for the two series over this 25-year sample is –0.68. NICHOLLS (1985) demonstrated the robustness of the relationship by calculating separate lag correlations for each ten-year data set from 1909 to 1982. For all seven 10-year subsets, the correlation coefficient between July–September pressure and subsequent October–April cyclone numbers ranged from –0.41 to –0.72.

However, NICHOLLS (1992) detected a sudden decrease in cyclone numbers within the region following the end of the 1985/86 season that has not been accompanied by a corresponding decrease in the Southern Oscillation Index (SOI). Thus, his method would have consistently over-predicted cyclone activity during the 1986/87–1990–91 seasons. This sudden change in the SOI-cyclone numbers relationship may have been a real physical change, or is perhaps a result of changes in satellite imagery interpretation, or inadvertent changes in the Southern Oscillation Index. NICHOLLS (1992) suggests that a possible remedy may be to correlate the trend in the SOI versus the change in cyclone numbers from one season to the next.

The second major work on seasonal prediction of tropical cyclone activity has been for the North Atlantic basin. Relationships between numbers of cyclones and the large-scale pressure patterns were originally found by NAMIAS (1955) and BALENZWEIG (1959). Major developments in documenting the predictability of this basin have been recently achieved (GRAY, 1984a, 1984b, 1990; GRAY et al., 1992, 1993; SHAPIRO, 1982a, 1982b, 1987, 1989). The number of tropical cyclones in a season has been related to various aspects of the large-scale flow, including the sea-level pressure, the patterns of sea-surface temperature, the upper-tropospheric zonal winds, and seasonal rainfall in the Sahel of West Africa. The strongest relationships have been with the Southern Oscillation and with the Stratospheric Quasi-Biennial Oscillation (QBO), which is a quasi-periodic reversal of zonal winds over the Equator. The tropical cyclone activity in seasons during the west phase of the QBO is a factor of 1.4 greater than during the east phase. Ascribing a simple index of +1 for a season in the west phase, 0 for transition seasons and –1 for east phase of the QBO, the correlation of this index with the cyclone numbers accounts for 33 % of the variance. Similarly, large correlations are found between cyclone numbers and an index of Southern Oscillation/El-Nino activity based on SST anomalies over the equator eastern Pacific.

Each of the above three forecast relationships for annual tropical cyclone activity included some aspect of El Nino/Southern Oscillation (ENSO) phenomenon as a key component.

NICHOLLS' forecasts for the Australian region are based completely on various indices of the Southern Oscillation. The correlation of cyclone numbers in the Australian region and the SOI in the months preceding the season is approximately 0.7 (i.e., accounting for 50 % of the variance). Perhaps the physical reason for the association is that the number of tropical cyclones during the season has a simultaneous high negative correlation with the large-scale surface pressure in the region; i.e., a low surface pressure is consistent with a large number of tropical cyclones. Since northern Australia is close to one of the centers of action of the Southern Oscillation, variations in this large-scale pressure are effectively equivalent to variations in the SOI. The predictability (or lag relationship) comes through the slow variation (or large serial correlation) of the SOI at the time of year preceding the Southern Hemisphere cyclone season.

During an ENSO warm event in the eastern Pacific, the pressure over Australia is high, which leads to a reduced number of cyclones in that region. REVELL and GOULTER (1986), HASTINGS (1990) and EVANS and ALLEN (1992) have pointed out that the frequency of cyclone formation at the eastern end of the Australian/South Pacific basin (i.e., east of 170E) actually increases during an ENSO warm event. Although the relationship between the formation longitudes in the region and the SOI is weak, it is statistically significant. However, the relationship appears to be dominated by the extreme events (i.e., warm events). If the relationship is real, the eastward movement of formation locations may be explained in terms of the favorable factors for cyclone formation discussed in Chapter 3.2. During an ENSO warm event, the region with SSTs exceeding 26° C extends much farther eastward across the South Pacific.

A number of authors has studied the association between the SOI and cyclone activity in the western North Pacific basin (ATKINSON, 1977; CHAN, 1985; DONG, 1988; ZHANG et al., 1990; LANDER, 1994). In each study, the simultaneous SOI relationship with the total number of cyclones over the basin has been quite weak. DONG (1988) suggested that the typhoon activity is suppressed by the El-Nino events in the basin west of 160° E but enhanced east of this longitude. Another study for northwest Pacific by AOKI (1985) shows the minimum frequency in typhoon formation during El-Nino events and maximum frequency two years later. CHAN (1985) reports that the number of cyclones east of 150 E increases when the large-scale pressure is high, i.e., during an ENSO warm event. The reason (given by CHAN) is the same as given above for the South Pacific. During an ENSO warm event, the monsoon shearline extends farther eastward than normal, which is a condition conducive for cyclone formation. This was extended by LANDER (1994) who showed that a large number of monsoon-shearline type cyclone formations occur late in the season of a warm event in a region east of 160E and south of 20E. Conversely during a cold event, no formations occur in that southern and eastward part of the basin.

The relationship between ENSO and cyclone activity in the North Atlantic basin apparently is quite different. It has been observed that El-Nino events reduce hurricane activities significantly in north Atlantic during the season following the onset of El-Nino and hurricane activity usually resumes to normal in the second summer following the events (GRAY, 1984a, 1988). Numbers of hurricane days are less by 60 % in moderate and severe El-Nino events in comparison to the non El-Nino years. The seasonal reductions in hurricane activity in the Atlantic in El-Nino years are reported to be due to the development of strong anomalous westerly zonal winds in the upper troposphere over the Lower Caribbean Sea and eastern Tropical Atlantic, which almost always occurred during the El-Nino years in comparison to the other years. SHAPIRO (1987) reports a correlation of –0.34 (only 12 % of the variance) between cyclone numbers and the warm water anomaly in the equatorial eastern

Pacific. Both SHAPIRO (1987) and GRAY (1984a) give evidence that the physical link is that higher equatorial SST values increase the activity of tropical convection, which increases the upper-level westerly zonal winds and the vertical wind shear downstream over the primary formation region of the Atlantic cyclones. As discussed above, large vertical shear represents an unfavorable condition for tropical cyclone formation (on this seasonal timescale).

The relationship between El-Nino events and tropical cyclone activities over northeast Pacific region are reverse to that of the Atlantic and northwest Pacific. It has been observed that in 5 El-Nino events since 1966 there is a strong indication that tropical cyclone activities have increased, especially, in the case of intense tropical storms. During El-Nino events, on the other hand, tropical cyclone activity is found to be suppressed over northeast Pacific.

Results for southwest Pacific (RAMAKRISHNA, 1989) appear to be interesting, as an enhancement in tropical cyclone activity has been observed in both the high and low phases of southern oscillation index.

The relationship between tropical cyclone behaviour and ENSO for North Indian Ocean has been examined by MANDAL (1989), but unlike the Atlantic and the Pacific, the relationship is found to be very weak. There is practically no change in frequency of the tropical cyclones during the ENSO episode in North Indian Ocean in comparison to the non El-Nino years or mean values.

8.5.2 Impact on Tropical Cyclone Tracks

GRAY (1984a, 1988) has shown that to some extent, El-Nino events also affect the intensity and track of the tropical storms in Atlantic. In El-Nino years the storms are less intense and more recurving over the Caribbean Sea. JOSEPH (1981) studied the motion of post-monsoon cyclonic storms over the Bay of Bengal with respect to years of highly deficient rainfall of India. JOSEPH (1976) pointed out that during the epochs of frequent drought years in all India monsoon rainfall, severe cyclonic storms of the Bay of Bengal of the post-monsoon season have preferred northward movement affecting Bangladesh and adjoining Indian coastal areas. A study by SINGH et al. (1987) for North Indian Ocean also shows some influence of southern oscillation on the latitude of the tracks of cyclones during post-monsoon season (October–December) crossing east coast of India. The above study also shows the increase in frequency of cyclones in low latitude (Andhra Pradesh coast) and the decrease in the higher latitude (Orissa and West Bengal coasts) during low phases of southern oscillation (El-Nino years). The study made by MANDAL (1989) for North Indian Ocean (NIO) has, however, shown that numbers of recurving and non-recurving tropical cyclones were found to be in almost equal proportion in El-Nino years. The study takes account of all the storms, which formed over the Bay of Bengal and Arabian Sea during a year (including monsoon season).

A notable study made by GUPTA and MUTHUCHAMI (1991) for the storms of Bay of Bengal region during post monsoon season (October–December) has shown significant relationship between El-Nino and the tropical storm tracks over the Bay of Bengal. The authors studied tracks of the storms during El-Nino and other years such as El-Nino (–1) years, El-Nino (+1) years and so on. After a careful analysis of the storm tracks in these years, it has been seen that the behaviour of storms tracks has some definite patterns during El-Nino and El-Nino (–1) years. While the storms tracks are mostly straight and less recurving during El-Nino years, they are more recurving during El-Nino (–1) years [Fig. 8.3 (a) & (b) and 8.4 (a) & (b)].

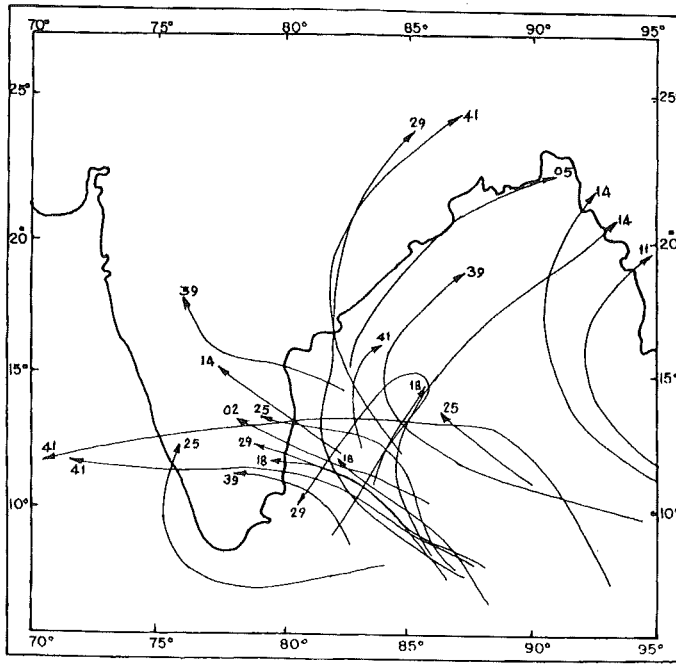

Fig. 8.3(a): Tracks of depression and cyclones over Bay of Bengal during post-monsoon season in El-Nino years (1901–1950). (Number written ahead of tracks indicates years of storm formation)

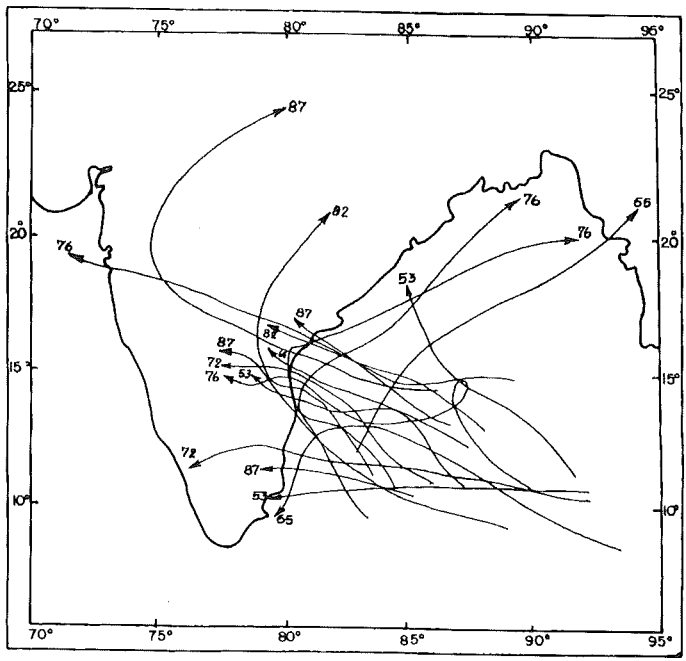

Fig. 8.3(b): Tracks of depression and cyclones over Bay of Bengal during post-monsoon season in El-Nino years (1951–1987). (Number written ahead of tracks indicates years of storm formation)

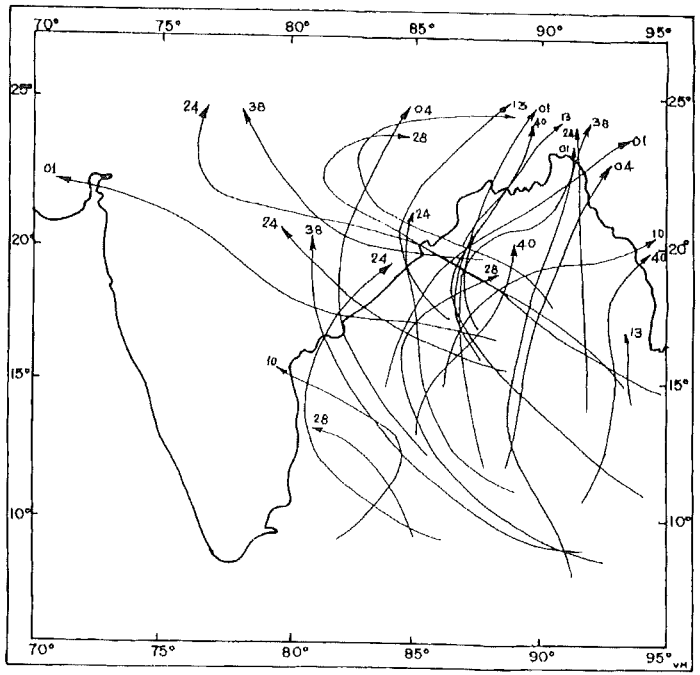

Fig. 8.4(a): Tracks of depression and cyclones over Bay of Bengal during post-monsoon season in El-Nino (–1) years (1901–1950). (Number written ahead of tracks indicates years of storm formation)

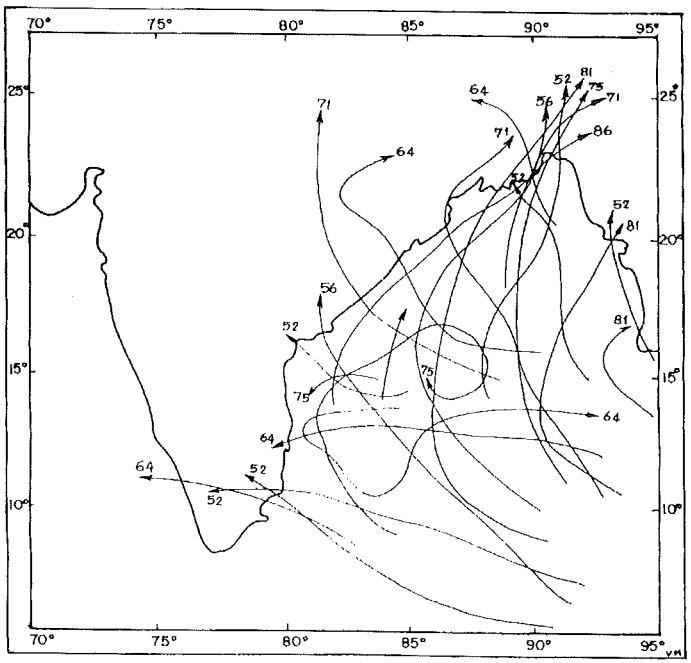

Fig. 8.4(b): Tracks of depression and cyclones over Bay of Bengal during post-monsoon season in El-Nino (–1) years (1951–1987). (Number written ahead of tracks indicates years of storm formation)

These results are opposite to those of GRAY (1984a, 1988) for Atlantic where the storms are found to be more recurving during El-Nino years. It is evident from these figures that El-Nino years have more numbers of storms crossing at lower latitudes on the Indian east coast compared to El-Nino (–1) years. To establish a quantitative approach to this behaviour, the storms were classified into two categories, viz., (1) recurving or those crossing north of 17° N and (2) non-recurving or those of which crossing south of 17° N on the east coast of India. There were mainly two considerations for choosing the latitude 17° N as the boundary between recurving and non-recurving systems. From the analysis of cyclone formation and their movement over the Bay of Bengal, it is observed that no cyclone forms north of 17° N during post-monsoon season and that maximum numbers of recurvature of the cyclones take place between the latitudes 15° and 17° N. Another observation was that almost all the storms crossing north of 17° N move north to northeastward during this season. Table 1 gives the details of the number of storms crossing Indian east coast under these two categories during El-Nino and El-Nino (–1) years. It may be seen from this table that 33 out of 38 tropical cyclones (about 87 %) during El-Nino years are non-recurving or crossing south of 17° N whereas 38 out of 48 tropical cyclones (about 79 %) during El-Nino (–1) years are either recurving or crossing north of 17° N. It may also be inferred from this table that during severe El-Nino years 15 out of 16 storms (about 94 %) have crossed south of 17° N whereas during years previous to these severe El-Nino years, 17 out of 19 storms (about 89 %) were either recurving or crossed north of 17° N.

To establish a correlation between the number of storms crossing south of 17° N during El-Nino years and the number of storm recurving/crossing north of 17° N during El-Nino (–1) years, fractional values of these numbers (n = 16) were statistically correlated and test of significance (t-test) was applied. The correlation coefficient of +0.84 was found between these two parameters, which are significant at 1 % level.

Although, considering past 87 years period (1901–1987) the total number of storms during 16 El-Nino years (38), as shown in Table 8.3, is less compared to the number in 16 El-Nino (–1) years (48), no preferred behaviour in terms of reduction or increase in the frequency of the storms is noticed in any kind of year [El-Nino, El-Nino (–1), etc]. Also, though characteristics of the storm tracks are distinctly different during El-Nino years compared to El-Nino (–1) years, but the prediction of onset of El-Nino based on the characteristics of the storm tracks in a particular year may not be possible as the storm frequency over North Indian Ocean is very low. On an average, 2 to 3 storms form over Bay of Bengal during post-monsoon season.

Table 8.3: Number of cyclonic storms recurving/crossing north of 17° N and those crossing south of 17° N during El-Nino and El-Nino (–1) years

El-Nino Years	No. of C.S.	No. of CS recurving/ crossing north of 17° N	No. of CS crossing south of 17° N	El Nino (–1) Years	No. of CS	No. of CS recurving/ crossing north of 17° N	No. of CS crossing south of 17° N
1902 (M)	1	0	1	1901	2	2	0
1905(M)	1	1	0	1904	1	1	0
1911(S)	1	1	0	1910	2	1	1
1914(M)	1	1	0	1913	4	3	1
1918(S)	3	0	3	1917	2	2	0
1925(S)	3	0	3	1924	5	4	1
1929(M)	3	0	3	1928	4	3	1
1939(M)	3	1	2	1938	3	2	1
1941(S)	4	0	4	1940	2	2	0
1953(M)	3	1	2	1952	7	4	3
1957(S)	0	0	0	1956	2	2	0
1965(M)	3	0	3	1964	4	2	2
1972(S)	3	0	3	1971	3	3	0
1976(M)	3	0	3	1975	3	3	0
1982(S)	2	0	2	1981	3	3	0
1987(M)	4	0	4	1986	1	1	0
Total	38	5	33		48	36	10
Mean	2.38	0.31	2.07		3.0	2.38	0.62
In %		13.1	86.9			79.2	20.8

C.S. = Cyclonic Storms; S = Severe El-Nino years; M = Moderate El-Nino years

The fractional values of storms crossing south of 17° N and southern oscillation indices (Tahiti-Darwin pressures) for the period 1901–1987 (n = 87) were statistically correlated and test of significance (t-test) was applied. The correlation coefficient of the –0.63 is found between SOI and storms crossing south of 17° N, which is significant at 1 % level. These results are in agreement with those of SINGH et al. (1987).

Similar studies for other basins are yet to be made available.

8.6 Possible Implications of Sea-Level Rise on Storm Surges

Projected sea-level rise due to global warming would inundate low lying areas, erode shore lines and destroy mangrove and Nepa palm forests. This would be particularly hard-felt in the deltaic regions where substantial area is barely above sea-level. Many coastal areas are at present submerging. Fig. 8.5 shows the sectors of the worlds' coast line that have been subsiding in recent decades, as indicated by the evidences of tectonic movements, logical and ecological indications, geodetic surveys, and groups of tide gauges recording a rise o mean sea level greater than 2 mm per year over the past three decades (BIRD, 1993).

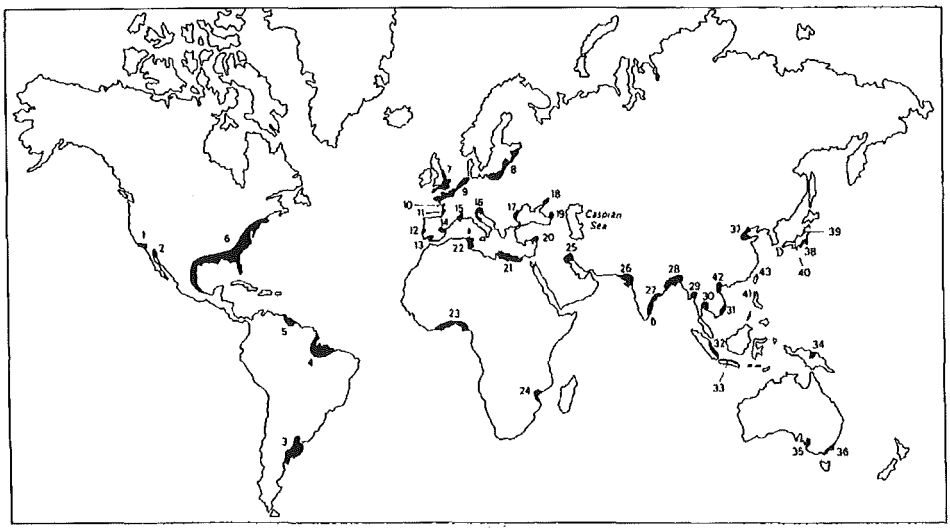

Fig. 8.5: Sectors of the world's coastline that have been subsiding in recent decades, as indicated by evidence of tectonic movements, increasing marine flooding, geomorphological and ecological indications, geodetic surveys, and groups of tide gauges recording a rise of mean sea level greater than 2 mm/yr over the past three decades (BIRD, 1993). 1, Long Beach area; 2, Colorado River delta; 3, Gulf of Laplata; 4, Amazon delta; 5, Orinoco delta; 6, Gulf and Atlantic coasts; 7, southern and eastern England; 8, southern Baltic coasts; 9, southern coasts of the North Sea and Channel coasts; 10, Loire estuary; 11, Vendée coasts; 12, Lisbon region; 13, Gaudalquivir delta; 14, Ebro delta; 15, Rhône delta; 16, northern Adriatic low coasts of Italy; 17, Danube delta; 18, eastern Sea of Azov; 19, Poti swamp; 20, southern Turkey; 21, Nile delta to Libya; 22, northeast Tunisia; 23, Niger delta and north coasts of the Gulf of Guinea; 24, Zambezi delta; 25, Tigris-Euphrates delta; 26, Rann of Kutch; 27, southern India; 28, Ganges-Brahmaputra delta; 29, Irrawaddy delta; 30, Bangkok coastal region; 31, Mekong delta; 32, eastern Sumatra; 33, northern Java deltaic coast; 34, Sepik delta; 35, Port Adelaide; 36, Corner Inlet region; 37, Hwang-He (Yellow River) delta; 38, head of Tokyo Bay; 39, Niigata; 40, Maizuru; 41, Manila; 42, Red River delta; 43, northern Taiwan

According to NICHOLLS and LEATHERMAN (1995), a 1 m sea level rise would affect six million people in Egypt, with 12 % to 15 % of the agricultural land lost 13 million in Bangladesh, with 16 % of national rice production lost, 72 million in China and tons of thousands of hectare of agricultural land. This could greatly increase existing storm surge threat because of the increase in the coastal area exposed to the surges originating in the sea, and loss of

coastal forests, which act as a buffer against the force of storm surges. The situation would be worse if the intensity and frequency of tropical cyclones increases due to warmer SSTs as projected by many workers.

Some conclusions drawn on the global vulnerability of storm surges due to sea level rise are (HOOZEMANS et al., 1993; BAARSE, 1995; IPCC, 1996):

(i) Some 200 hundred million people are estimated to live currently below the highest storm surge level (the once-per-1000-years storm surge level). Based on this population estimate, as well as on first order estimate on storm surge probability and existing level of protection, 46 million of people are estimated to experience flooding due to storm surge in an average year under present condition. Most of these people live in the developing countries.

(ii) The figure will double if the sea level rises 50 cm (92 million people per year) and almost triple if it rises 1 m (118 million people per year).

(iii) Because of regional differences in storm surge regimes, the increase of flood risk due to sea level rise is greater than average for the Asian region (especially in the Indian Ocean Coast), the south Mediterranean coast, the African Atlantic and Indian Ocean Coasts, Caribbean Coasts and many of the small islands.

The surges are superimposed on raised mean sea level (MSL). In view of the dynamical effects in a shallow coastal area, the components of total water level due to storm surge, astronomical tide and MSL are mutual dependent and interact dynamically with each other. Therefore, for estimating the total water level one cannot assume that MSL, tide and surge are linearly additive and there is no non-linear interaction.

There are two important issues associated with implication of sea-level rise on storm surges. Firstly, raised mean sea level implies greater potential inland inundation due to storm surges and in second place higher mean sea level may itself affect the surge and tidal components of the rise. Another issue, which has attracted attention, is related to the sensitivity of storm surges to change in projected cyclone intensity as a result of changes in SST. In the following section we will briefly discuss these issues and describe attempts made by various workers to address the problems of different vulnerable regions.

8.6.1 Bay of Bengal

Storm surges in the Bay of Bengal are the major cause of coastal flooding along the east coast of India and Bangladesh. In the context of the projected rise in the sea level due to green house warming, it may be interesting to examine how changes in mean sea level (MSL) may affect the storm surges and consequently the coastal flooding in the Bay of Bengal.

As mentioned earlier, low lying coastal regions of Bangladesh are worst affected due to storm surges. Exposure of population to sea level rise and storm surges is particularly an extremely grave consideration in Ganga-Brahmaputra-Meghna delta of Bangladesh. Local subsidence in this region is very significant which may increase the relative rate of sea-level rise. Ganga-Brahmaputra-Meghna river systems together deliver approximately 1.6 billion tonnes of sediments annually (MILLMAN and MEADE, 1983). The damming of Meghna River could prevent sediment influx from compensating for local subsidence, increasing coastal erosion. Thus making the problem of coastal flooding due to storm surges and MSL more serious.

BROADUS et al. (1986) and BROADUS (1993) have made a detailed study of the possible effect of sea level rise and damming of rivers in the coastal areas of Bangladesh and Egypt.

The potential economic implications of two relative sea levels rise scenarios for the year 2050 and 2100 has been examined.

Table 8.4 gives these scenarios of relative sea level rise for Bangladesh together with the economic activities/assets in affected areas (BROADUS, 1993).

Table 8.4: Relative Sea Level Scenarios and Economic Activities/Assets in Affected Areas of Bangladesh

Activities/ Assets	1 m (2050)	3 m (2100)
Total sea level rise	0.83 m	3.4 m
(Global)	(0.13 m)	(2.2 m)
(Local subsidence)	(0.70 m)	(1.2 m)
Loss habitable land	7 %	26 %
Population	5 %	27%
Gross Domestic Product (GDP)	5 %	20 %

Fig. 8.6 gives the landward transgression scenarios from a 1 m, 2 m, 3 m, and 5 m rise in relative sea level. The 1 m and 3 m scenarios correspond to the projected 13 cm and 2 m of global sea level rise by 2050 and 2100 respectively. It may be seen from these scenarios that even with 1 m relative sea level rise large population and economic activities will be exposed to serious threats from storm surge flooding. Percentage of population lying between 1 m and 3 m transgression lines is very high which includes the city of Khulna having population density more than 29000 per km^2 (BROADUS, 1993).

Another significant consequence of the relative sea level rise pointed out by BROADUS (1993) is the loss of Sunderban Forest Reserve in Khulna district which at present provides vital protection for this area by acting as a buffer against storm surges. Loss of this buffer could increase the threat of storm surge floods, which could reach up to greater inland distances.

DUBE and RAO (1989, 1991) used a continuously moving coastal boundary numerical model to examine how changes in MSL may affect the storm surges and the low lying coastal flooding along the east coast of India. The authors have presented different scenarios indicating the implication of a rise in the sea level on the surge generated by the 1977 Andhra cyclone. Authors found that higher MSL of the Bay of Bengal allows the storm surges to build on a higher base with increased inland inundation along the low lying regions of Andhra coast of India.

Using a numerical storm surge model FLATHER and KHANDKER (1993) examined the effect of rise in mean sea level on tides, storm surges and their interaction for the Bay of Bengal. They simulated the surge generated by the Bangladesh cyclone of May 24–25, 1985 with and without 2 m rise in sea level. For the M2 tides, authors found an increase in amplitude by 10 cm in NE and decrease by similar amount NW of the Bay when the sea level is raised by 2 m. For the storm surge a reduction in the maximum computed surge elevation of 20–30 cm was predicted by a 2 m rise in MSL (Fig. 8.7). Authors attribute this to a decrease in the ratio, wind stress/water depth that occurred in the case of an elevated MSL, which is also consistent with theory and other model studies. Tide-surge interaction response with raised MSL resulted in a reduction of maximum computed water level in the NE and NW corners of the Bay, with an increase in level in an area between (Fig. 8.8 a, b). Authors attribute this more

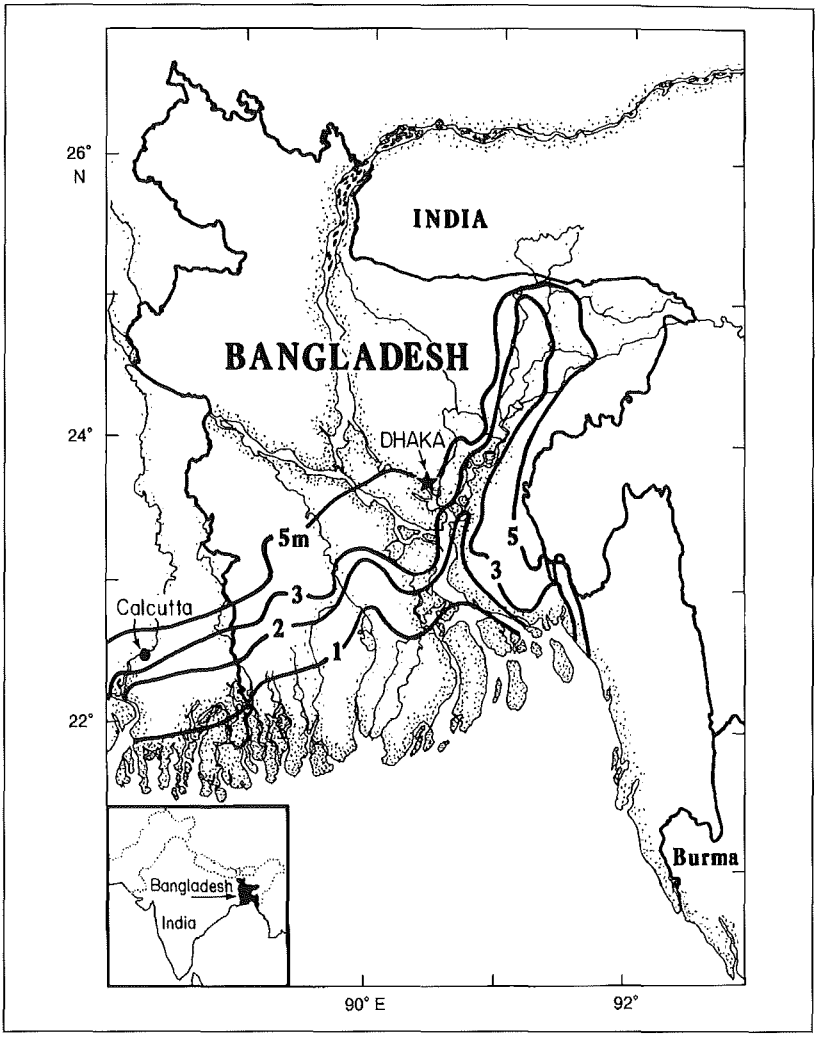

Fig. 8.6: Sea level transgression scenarios for Bangladesh (BROADUS, 1993)

complex behaviour to the variations in the relative timing of tidal high water and peak surge. FLATHER and KHANDKER (1993) further noted that a reduction of 20 cm in maximum computed water level suggests that the effect of the 2 m increase in MSL would be to raise the highest flood level by about 1.8 m above those expected with the present MSL.

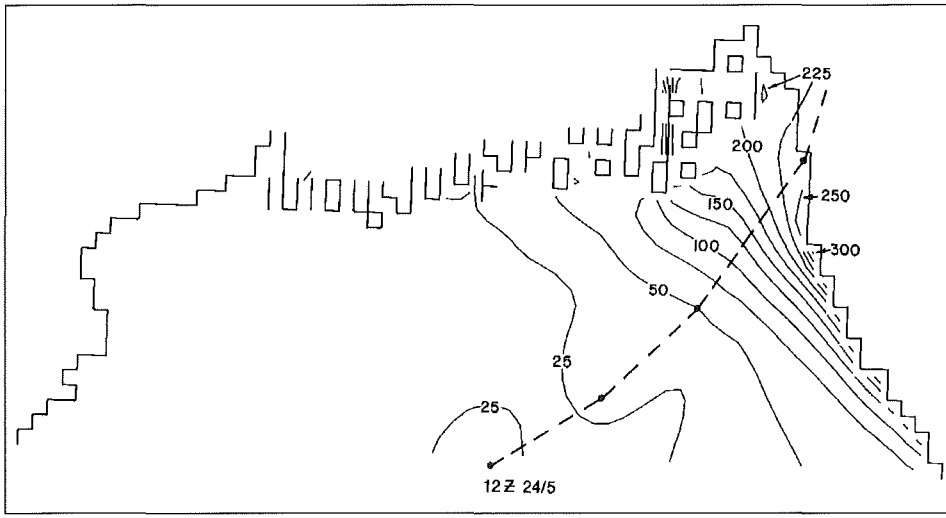

Fig. 8.7(a): Contours of maximum computed surge elevation (cm) in the period 1200 GMT 24 May to 1200 GMT 25 May 1985. The broken line indicates the track of the cyclone
(FLATHER and KHANDKER, 1993)

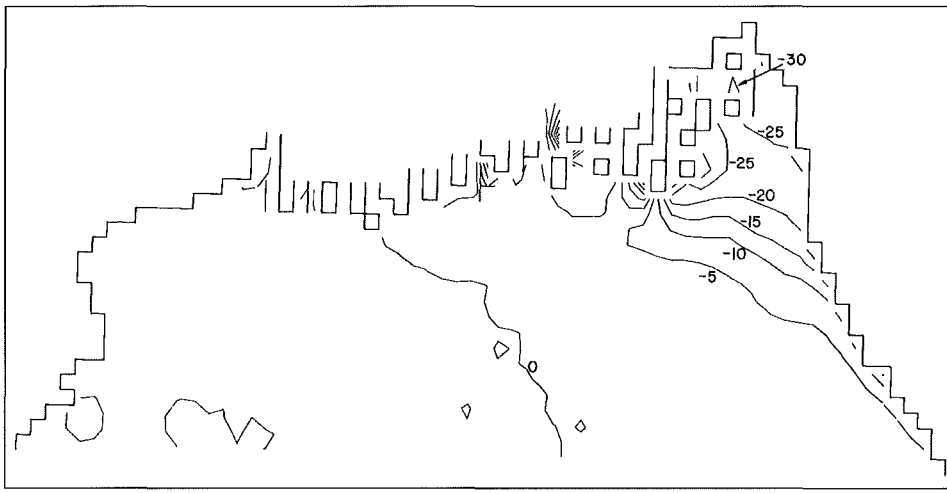

Fig. 8.7(b): Change (cm) in maximum computed elevation (cm) produced by a 2 m rise in MSL
(FLATHER and KHANDKER, 1993)

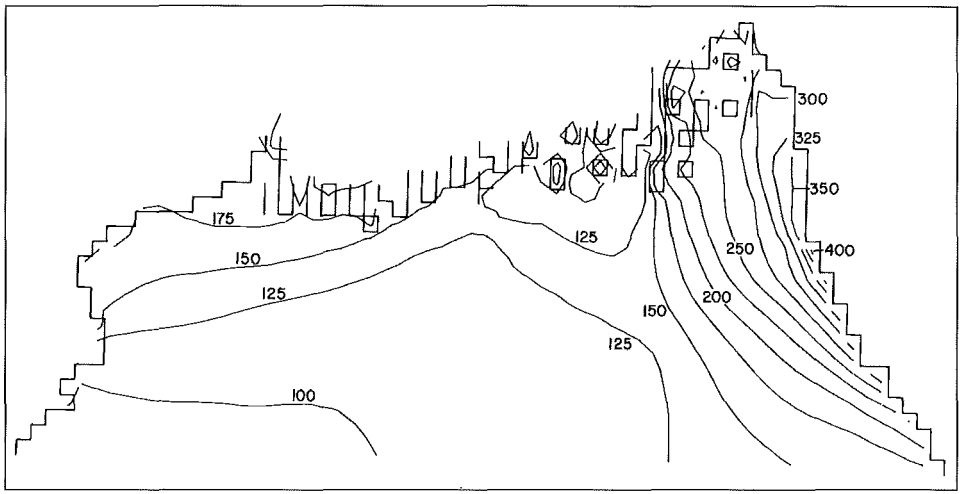

Fig. 8.8(a): Contours of maximum computed elevation (cm) due to tide and surge in the period 1200 GMT 24 May to 1200 GMT 25 May 1985 (FLATHER and KHANDKER, 1993)

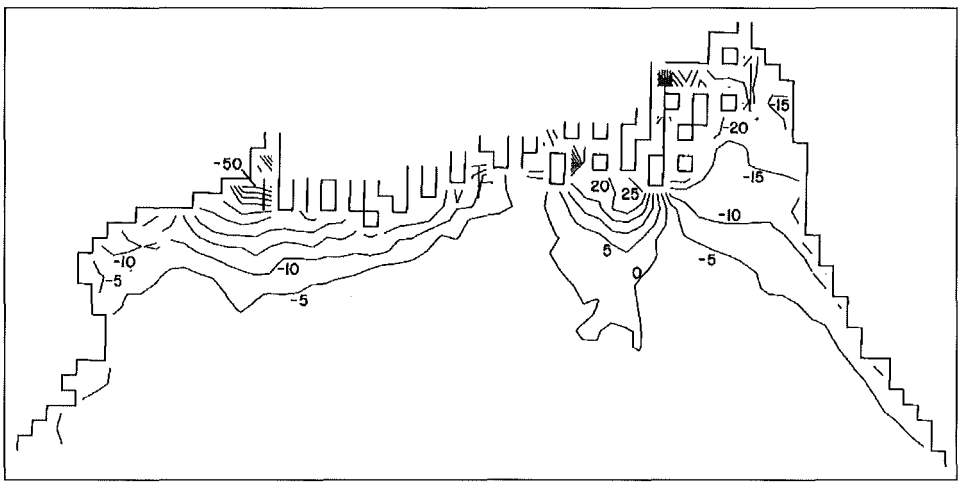

Fig. 8.8(b): Change (cm) in maximum computed tide + surge elevation produced by a 2 m rise in MSL (FLATHER and KHANDKER, 1993)

ALI (1996) used a numerical model to generate storm surge scenarios for Bangladesh under increased cyclone intensity and sea level rise. Using the temperature and wind relation given by EMANUEL (1987), the likely wind speeds of the April 1991 cyclone that hit Bangladesh under two sea surface temperature scenarios of 2° C and 4° C have been estimated by the author. These wind speeds were then used to compute storm surges for a sea surface temperature rise of 2 and 4° C, and sea level rise of 0.3 and 1.0 m. Surge heights computed by ALI (1996) under these conditions are given in Table 8.5. Numbers in parentheses indicate percentage increase or decrease in storm surge heights from the present surge height. It may be seen from the table that a rise in the sea level tends to reduce storm surge heights which is on expected lines as the increase in sea level results in increased water depth over the continental shelf. On the other hand a maximum increase of about 49 % in the surge height is predicted for the increased intensity of cyclone corresponding to a 4° C rise in SST.

Table 8.5: Storm surge heights (m) under different sea surface temperatures and sea level rise scenarios (wind speed of 225 km h^{-1} corresponds to that of the April 1991 cyclone) (ALI, 1996)

	Current Temp. (27° C)	2° C Increase	4° C Increase
Wind (km h^{-1})	225	248	275
No Sea Level Rise Surge Height (% change)	7.6 (0 %)	9.2 (21 %)	11.3 (49 %)
Sea Level Rise = 0.3 m Surge Height (% change)	7.4 (–3 %)	9.1 (20 %)	11.1 (46 %)
Sea Level Rise = 0.1m Surge Height (% change)	7.1 (–7 %)	8.6 (13 %)	10.6 (40 %)

ALI (1996) also used an empirical formula to compute inland inundation along flat land around Meghna estuary associated with April 1991 cyclone under the present and warmer SST conditions. He found increased inland penetration of the surge by 13 % and 31 % for a SST rise of 2° C and 4° C respectively. In conclusion author considers these results as indicative only because of several simplifying assumptions, which are used, and uncertainties concerning the relationship of SST's and cyclone intensities.

In a recent study SINHA et al. (1997) applied a tidal circulation model to examine how a sea level rise might affect the water level and currents in the Hooghly estuary situated in the head Bay of Bengal. For this study the authors did not consider the changes in the shoreline as a result of rise in sea level. Model results show a substantial increase in the amplitude and velocities of the tidal wave due to the sea level rise by 50 cm and 1 m in Hooghly estuary. Results also indicate that variations in the tidal wave due to raised mean sea level become more prominent in the upstream regions of Hooghly estuary. Magnitude of tidal currents is also found to increase significantly with rise in sea level. The results are important as they suggest that these changes in the flow field of Hooghly estuary may increase the salinity intrusion. Besides the increase in currents due to sea level rise may cause more erosion of banks of estuary, shifting the net deposition further northward.

8.6.2 Arabian Sea and Maldives

The threat from sea level rise and storm surges is not a serious consideration in most parts of the west coast of India, coast of Pakistan, Arabian/Persian Gulf, Saudi Arabia, Red Sea and east coast of Africa. The only region that is vulnerable to severe storm surge is the Gujarat coast of India. While projected sea level rise of 50 cm to 1 m by 2100 is expected to affect hundreds of thousands square kilometers of coastal wetlands and low lands in these countries, many small island countries face a bigger threat as they could loose a significant part of their land area.

The problem is particularly acute in the Maldives, which is in southern part of the Arabian Sea. The Maldives archipelago consists of 1,190 islands stretched in a chain 820 km in length extending from Ihavandiffula (6° 57'N) to Addu Atoll (0° 34'S). The average elevation of these islands is 1 to 1.5 m above existing sea level (PERNETTA, 1992). Much of the island, and almost all the village, is 0.8–1.1 m above mean sea level.

Tropical storms are rare in Maldives, but increase in occurrence and intensity towards the north. Storms are experienced on Minicoy, and Lakshdweep Islands of India, which are to the north of Maldives. The tidal range is up to 1.2 m in the north and 1.4 m in the south of Maldives. Occasional storms accompanied by high astronomical tides cause destructive flooding in islands. In fact, flooding is the major concern as 80 % of the nation's land area is less than 1 m above sea level. Particularly affected has been the capital Male' which is heavily crowded with over 70,000 people inhabiting the 1.8 sq. km area. Due to large population pressure the island has been extended in all directions, and the combinations of all reclaimed shoreline and mined reef, have increased the vulnerability of Male. This was especially the case on 10–12 April 1987 when Male' experienced high waves which inundated much of the island.

Rising sea levels would almost certainly cause most of the islands to become uninhabitable, displacing more than 225,000 Maldivians. In fact, a rise of one meter sea level would sink about 80 % of the Maldives beneath the sea.

In conclusion we may say that although storm surge is not a threat to Maldives, the nation stands to loose heavily from the adverse effects of global warming and sea level rise.

Lakshadweep Islands of India are also vulnerable to sea level rise. Anticipated rise of sea level by 1m may cause heavy land loss in Kiltan, Kaviratti, Kadmat, Kalpani, Cheriyan and Agati-Bingaram Islands (NIGAM, 1989).

8.6.3 Persian Gulf, Red Sea and the Mediterranean Sea

The Persian Gulf region is mainly influenced by extra-tropical weather systems, whereas the region south of the Strait of Hormuz is affected by tropical cyclones. The Gulf is subjected to major negative and positive storm surges. Particularly vulnerable to sea level rise in the Persian Gulf is the region Tigris-Euphrates delta (Fig. 8.5), which is characterised by negative surges (EL-SABH and MURTY, 1989). Impact of sea level rise on storm surges, therefore, does not appear to be a threat in the Persian Gulf. On the other hand, there is no present indication of rising sea level in Red Sea.

Regions, which are vulnerable to sea level rise in Mediterranean, are Ebro delta, Rhone delta, northern Adriatic low coasts of Italy, Danube delta, eastern sea of Azov, Poti Swamp, Southeast Turkey, Nile delta of Libya and northeast Tunisia. Regionally, Southern Mediterranean appears to be most vulnerable to sea level rise (Fig. 8.5).

BROADUS (1993) made a detailed study of the impact of projected sea level rise in the deltaic regions of Nile River in Egypt. Scenarios of exposure of population and economic activities relative to sea level rise of 1 m by 2050 and 3 m by 2100 is presented by the author. The analysis suggests that a 1 m rise in sea level (including local subsidence) would cover areas currently accounting for about 12 % of habitable land, 14 % of population and 14 % of Gross Domestic Product (GDP) in Egypt. The figures corresponding to 3 m rise are much higher. Storm surge is not a problem in Egypt; however, with rising sea level the region is likely to be frequently flooded due to waves and tides in the Mediterranean.

8.6.4 European Seas

The regions which are vulnerable to sea level rise in Europe are: Southern and Eastern England, Southern Baltic Coast, Southern Coast of the North Sea and Channel coasts, Loire estuary, Vendée coasts, Lisbon region and Gaudalquivir delta (Fig. 8.5). From the storm surge point of view the North Sea region is of importance and concern and therefore, has been investigated by many workers.

A two-dimensional hydronamic model of the North Sea and part of the continental shelf was used by DE RONDE (1993) to calculate the tidal system changes as a result of arbitrary sea level increase of 2.5 and 5.0 m. He considered the Netherlands' complex coast in detail for his study. The author also examined impact of sea level rise on storm surge. Some of the conclusions reached by DE RONDE (1993) for the case of a 1 m sea level rise are:

(i) 0.95–1.1 m rise in mean high water level with insignificant changes in the tidal motion in the North Sea and along Dutch coast.
(ii) Less than 5 cm change in storm surge amplitudes.

JELGERSMA et al. (1995) examined in detail the Holocene storm surge signatures in the coastal dunes along the central Netherlands' coast. They describe and discuss the occurrence and possible significance of Holocene shell deposits, which have been found intercalated in the dune sands. These deposits are believed to be the result of storm surge activity on the foreshore, either through swash or over wash action, and of subsequent preservation due to aeolian coverage of basically sedimentry coastal system. Taking into account of the contemporary mean sea level, the authors gave an interpretation of the surge level elevations associated with the depositions. Authors found an increasing level of storm surge elevations with increasing time. They suggest that climatic variations on the one hand and foreshore bathymetry on the other hand may be factors of relevance to explain these results.

Several observational and modelling studies have been carried out to examine changes in mean sea level on the German Baltic coast and German Bight of North Sea. Mention may be made of some of the recent observation and studies in this regard (SIEFERT, 1990; HOFSTEDE, 1991; SIEFERT and JENSEN, 1993; TOPPE, 1993; PUNNING, 1993; KUNZ, 1993, STIGGE, 1993). Almost all of these studies confirm a rise in mean sea level on both the Baltic and North Sea coast of Germany. Fig. 8.9 shows that observed MSL and its trend at Cuxhaven, (Germany).

STIGGE (1993) investigated sea level changes and high water levels probability on the German Baltic coast with the purpose of defining the defence level (maximum high water crest) for the next fifty years. An accelerated rise of storm surge frequency during last 50 years was observed (Fig. 8.10). He notes that a rise in MSL could produce an increase in the storm

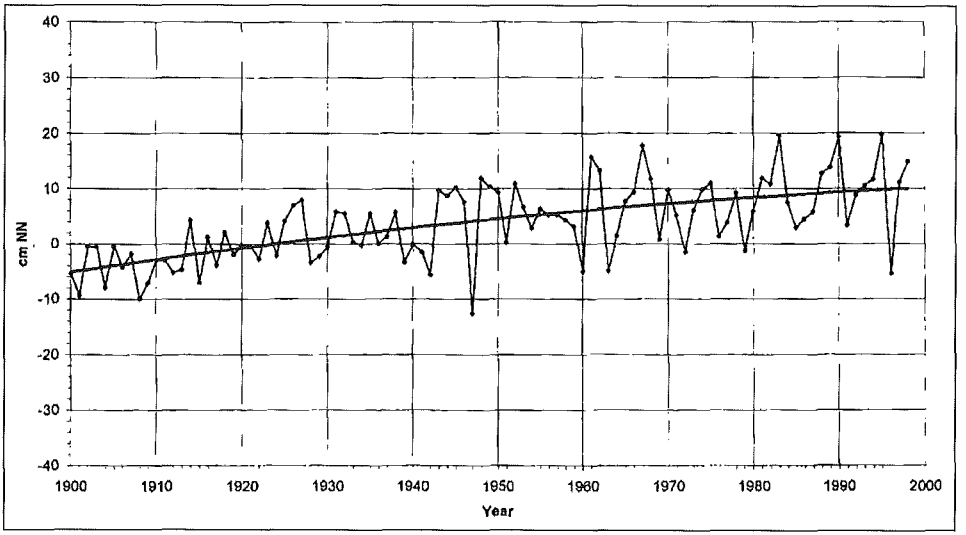

Fig. 8.9: Mean Sea Level at Cuxhaven (FERK, 1999)

surge frequency both in the North Sea and in the Baltic Sea. At first glance a differentiation between these two cases seems of little importance, but it may be noted that storm surges can be influenced by stronger winds associated with intense cyclones, in addition to the effect of a slow rise in MSL. STIGGE (1993), therefore, did not accept the widely held opinion that an increase of storm surge frequency in the western Baltic necessarily has to be connected with a significant increase of the high water crests.

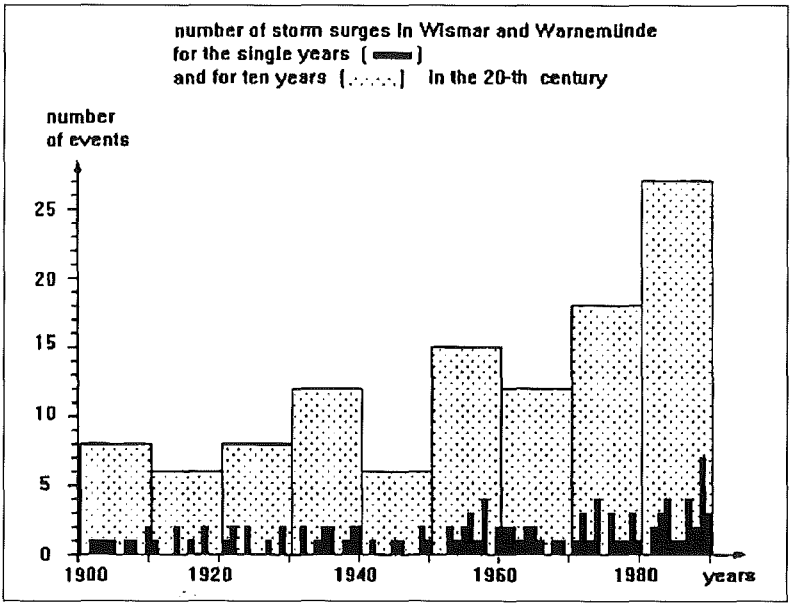

Fig. 8.10: Frequency of storm surges on the German Baltic coast (STIGGE, 1993)

8.6.5 The Americas

Sectors of the American coastline which are particularly vulnerable to relative rise in mean sea level are Long Beach area and Colorado River delta on the Pacific coast and Gulf of La Plata, Amazon delta, Orinoco delta, Gulf of Mexico on the Atlantic coast (Fig. 8.5).

Impact of sea level rise on coastal systems of Mississippi River deltaic plain in the Gulf of Mexico was examined by DAY et al. (1993). Mississippi delta consists of lakes, bays, near sea level wetlands and low-lying uplands. Water levels in this region have increased substantially, primarily from regional land subsidence rather than eustatic sea level rise. Because of continuing subsidence and apparent sea level rise, many low-lying areas are experiencing increased flooding from the river and from the sea (during storm surges).

New England is not frequently visited by hurricanes; however, severe hurricanes about once a decade strike Southern New England. If sea level continues to rise as a result of global warming, the destruction wrought by future storms could wipe out many seaside oases. In the event of a severe hurricane striking the coast, the rise in the sea level would be compounded by a storm surge that would make high 10 to 15 feet water level some to higher than usual (ALLEN, 1998). ALLEN (1998) further indicates that severe hurricanes like the one that struck New England three times between 1938 to 1954 may generate very large amplitudes the storm surge.

Impact of sea level rise on the east coast of south America has been examined in detail by LEATHERMAN (1986) and SCHNACK (1993). This coast is not vulnerable to severe tropical cyclones and storm surges.

8.6.6 Australia

LOVE (1988) derived a number of tropical cyclones storm surge climatologies for three Australian parts, Darwin, Mackay and Port Hedland. For his analysis he considered the present climatological scenario and the scenarios after specifying possible responses of the tropical cyclones climatology to a SST warming of the order of 1.0 °C in the oceans surrounding northern Australia accompanied by a sea level rise of 1 m. He demonstrated that sea level rise will have a significant impact on estimates of the return periods for extreme surge events, shortening them at all the three locations (i.e., the frequency of surge events is increased). Table 8.6 gives the return period of tropical cyclone storm surges of 5 m, 2.5 m and 4 m above high astronomical tide (HAT) at Port Hedland, Darwin and Mackay respectively.

Table 8.6: Return period (in years) for tropical cyclone storm surges above specified level for the three selected ports under a variety of warm climate scenarios (LOVE, 1988)

	Port Hedland	Darwin	Mackay
Surge level above HAT	5 m	2.5 m	4 m
"Present"	13 000	36 000	16 000
"Present" plus 1 m sea level rise	1000	4100	600
Increase "Frequency" of cyclones plus 1 m sea level rise	900	1800	650
Increased "Intensity" of cyclone plus 1 m sea level rise	430	650	200
Increased "Frequency" and "Intensity" cyclone plus 1 m sea level rise	350	450	180

MCINNES and HUBBERT (1995) used a sophisticated storm surge model capable of simulating the inundation associated with May 1994 and November 1994 mid-latitudes severe storms of Port Phillip Bay in the southeast pait of Australia. They performed three experiments: (i) Exp 1: Controlled experiment, (ii) Exp 2: Sensitivity experiment with increased sea level rise of 80 cm, and (iii) Sensitivity experiment with 10 % increase in the wind forcing in addition to a sea level rise of 80 cm. Results were presented for the entire Port Phillip Bay as well as the three small domains Werribee, Hobson's Bay and Mordialloc. They found different order of inundation in these three areas, leading to the conclusion that the estimation of the climate impact in the coastal region is highly site-specific problem. The areas of inundation in each of the three regions increased with the increase of sea level and with a further inundation with 10 % increase in wind strength (Table 8.7).

Table 8.7: Summary of the ratio area inundated to the area of inundation in Exp. 1 for the same event and model domains. The three domains are Werribee (W), Hobson's Bay (HB) and Mordialloc (M). The value in brackets denotes the total area inundated in km^2 (PITTOCK et al., 1996)

	May 1994			Nov. 1994		
	W	HB	M	W	HB	M
Exp. 1	1.0 (11.2)	1.0 (0.9)	1.0 (0.7)	1.0 (15.8)	1.0 (0.9)	1.0 (0.7)
Exp. 2	2.7 (30.4)	1.9 (1.7)	9.3 (6.5)	2.2 (34.4)	2.0 (1.8)	8.9 (6.2)
Exp. 3	3.1 (34.3)	2.6 (2.3)	11.0 (7.7)	2.6 (41.0)	3.2 (2.9)	12.6 (8.8)

PITTOCK et al. (1996) made a detailed review of the effect of enhanced green house on the climatology of tropical cyclones. They also reviewed the changes in storm surges due to tropical and extra-tropical cyclones as a result of mean sea level rise. They highlighted the requirement of site-specific inundation modelling studies as the magnitude of increase in coastal inundation due to rise in mean sea level heavily depends upon the specific characteristics of the site, including both meteorology and coastal geomorphology. More recently HUBBERT and MCINNES (1999) developed a high resolution storm surge inundation model

for coastal planning and impact studies. Model simulations were successfully carried out for the town of Port Hedland on the northwest coast of Australia and for the Port Phillip Bay, upon which the city of Melbourne is located. Scenarios of sea level rise and increased storm wind strength were imposed on the model simulations to explore the possible impact of climate change on two potentially vulnerable regions in south eastern Australia as well as demonstrate the application of the model to impact studies of this kind.

8.6.7 China

China has extensive coastal low lands with three great deltas of Yellow River, Yangtze River and Pearl River. Although all these deltaic regions are vulnerable to sea level rise, the Yangtze River deltaic plain is most vulnerable to accelerating sea level rise.

REN (1993, 1994) made a detailed study of sea level rise and its impact on coastal regions of China. The most significant impact of future sea level rise will be the increased vulnerability to sea inundation of coastal low land due to storm surges. Heaviest casualties ad loss of property from storm surges in China occur in the Yangtze River delta. Shanghai area especially experiences enormous losses as a result of combination of flood, astronomical high tidal level and typhoons.

Rising trends in storm surge levels of Shanghai area is currently indicated by observations (YANG, 1996). ZHU and XIE (1995) used a numerical model to compute tidal current and storm surges in the Yangtze River estuary for a projected sea level rise of 50 cm. According to the results of numerical calculations, slight decrease in surge amplitude is seen with a rise in sea level (average decrease in 9 cm in the northern coast and 6 cm in the southern coast of the Yangtze River). Although, the effect of sea level rise is small, the probabilities of occurrence of the storm surge level at a given height will have significant increase due to raised initial mean sea level. Table 8.8 gives the storm surge level with different probabilities of occurrence in the Yangtze River deltaic plain (YANG, 1996).

More recently QIN (1997) used a numerical storm surge and tide model to estimate the impact of sea level rise in the coming decades on the storm surges and tides in Shanghai regions. He estimated a mean annual relative sea level rise of 15–20 cm by 2010, 25–35 cm by 2030 and 40–50 cm by 2050 in Shanghai region as compared to unaltered sea level in 1990. To examine the impact of relative sea level rise on storm surges and tides, QIN (1997) used six severe tropical cyclones hitting Shanghai region. The effect of sea level rise on the storm surges at Wusong is shown is Fig. 8.11. It may be seen from the figure that the amplitude of storm surge decreases with increasing sea level. The maximum effect of the sea level rise on the storm surges in 2010, 2030, and 2050 relative to 1990 could be –0.5, –2.5, and –5.0 cm respectively.

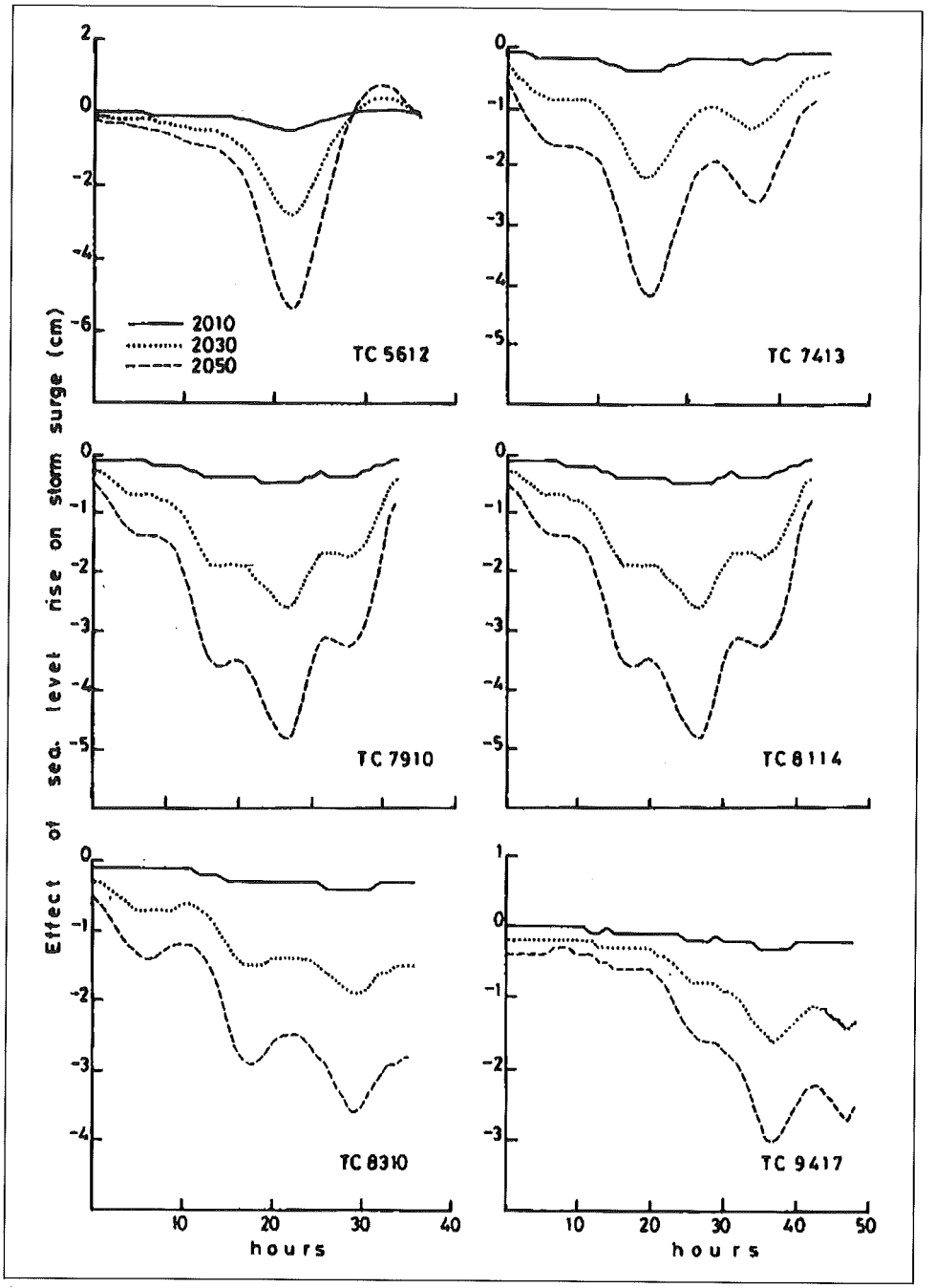

Fig. 8.11: The effect of sea level rise on the storm surge at Wusong (QIN, 1997)

Table 8.8: The impact of sea level rise on storm surge in the Yangtze River deltaic plain (Wusong Datum Plane, m) (YANG, 1996)

Coast section	SLR (cm)	Storm surge level with different probabilities of occurrence					
		1/5	1/10	1/20	1/50	1/100	1/1000
The southern coast	0	5.02	5.17	5.32	5.54	5.69	6.24
The northern	50	5.46	5.61	5.76	5.98	6.13	6.68
coast	0	4.22	4.45	4.68	4.96	5.17	5.88
	50	4.63	4.86	5.09	5.37	5.58	6.29

This negative effect was expected as the rise in sea level results in the decrease of local wind set up and deeper local water than the initial one which leads to decrease of storm surge amplitude. Regarding impact of future relative sea level rise on tides, he found that tides exhibit periodic variations with the same periods as that of tide. The effect increases with increasing rise in relative sea level and retains its period unaltered.

WANG and WANG (1997) calculated maximum storm surge elevations with certain return periods for Guangdong Province of China. They used joint probability method to compute maximum elevations.

Hong Kong is threatened by the possibility of inundation from the sea whenever a tropical cyclone approaches. A number of studies has been carried out in the past (WATTS, 1959; CHENG, 1967; PETERSEN, 1975; LAU, 1980b; CHAN, 1983; CHAN and CHANG, 1997) on maximum sea level during storm surges. Sea level has been rising at an average rate of about 0.3 mm/yr in Hong Kong (YIM, 1993). It is estimated that as a result of global warming sea level may rise 31–110 cm by the year 2100. This will have major environmental effects on coastal lowlands, especially low-lying land reclaimed from the sea in Hong Kong. Although presently there is no evidence for an increase in the frequency of storm surges which may be the result of a rising sea level, Hong Kong is facing a continuing, and perhaps increasing risk of marine inundation from tropical cyclone surges.